Canadian Journal of Pure and Applied Sciences
Vol. 16, No. 3, pp. 5505-5514, Oct 2022
Online ISSN: 1920-3853; Print ISSN: 1715-9997
Available online at www.cjpas.net

ON THE AZIMUTHAL DEPENDENCE OF ORTHORHOMBIC FRACTURES FOR VERTICAL SEISMIC PROFILES USING THE ELLIPSOIDAL APPROXIMATION

Pedro Contreras
Department of Physics, University of Los Andes, Mérida, 5001, Venezuela

ABSTRACT

The analysis of travel times with moveout velocities represents one of the most widely used seismic signal processing techniques for the exploration and monitoring of oil and gas reservoirs. In travel time analysis for anisotropic elastic media with fractures, the knowledge of the conversion point at interfaces with incident longitudinal and reflected transversal elastic response impulses taking into account the azimuthal dependence is important for both seismic data analysis acquired in multicomponent surveys and the correct interpretation of seismic in reservoirs. Henceforth, this work shows how to derive analytical expressions for the longitudinal to transverse response impulse "P-S_i" conversion points using the ellipsoidal approximation for fractured orthorhombic elastic media under kinematical considerations. These expressions can be used for vertical seismic profiles with small polar angles of aperture and azimuthal dependence in orthorhombic media when the elastic slowness is used as a main theoretical tool to resolve the Christoffel equation. We also explain some of the differences within the ellipsoidal inversion procedure of the elastic stiffnesses C_{13} and C_{23}.

Keywords: Vertical seismic profiles, ellipsoidal approximation, orthorhombic anisotropy, P-S_i conversion points, azimuthally dependent elastic media.

INTRODUCTION

In seismic oil and gas exploration, one of the most important theoretical tools to start with any analysis that involving the direct task of finding the elastic velocity field to infer lithology properties, the inverse estimation of the elastic stiffness tensor field and the fracture orientation is the Christoffel equation (Grechka, 2017; Musgrave, 1970). The Christoffel equation can be resolved to initially give the eigenvalues and eigenvectors that represent phase velocities and phase angles for all the elastic symmetries (Musgrave, 1970) (the symmetries of anisotropic rocks in seismic are a subgroup of the symmetries found in the Bravais lattice, namely the hexagonal (VTI), the orthorhombic, the monoclinic, and the triclinic ones. They are called low symmetry systems and with the subsequent estimation and visualization of the group velocity elastic field (also called response impulses field) and their corresponding angles calculation (see a-panel in Fig. 1). Thomsen (1986) serve as the main tool for what is called the forward modeling of the Earth's crust in Exploration Geophysics. This procedure finds practical applications in VTI media with a vertical axis of symmetry (Thomsen, 1986), and also in azimuthally dependent (Tsvankin and Grechka, 2011) fracture media such as the HTI (Contreras *et al*., 1999), the orthorhombic (Grechka and Tsvankin, 1997) and the monoclinic elastic fractured systems (Hao and Stovas, 2014). However, there are additional issues on how to apply the elasticity formalism derived from the Christoffel equation to seismic exploration.

The first factor to consider is the acquisition geometry if the acquisition has wider angles of apertures with a surface source and geophones arrangement, or on the other hand, vertical seismic profiles (VSP) with a surface source and downhole geophones. This is a practical issue since it takes into consideration the data acquisition and processing in geophysical exploration and monitoring analysis of oil wells. It can in principle be used sources with P waves and additionally use the transversal waves generated at the interface when the elastic energy converts from one to another elastic mode ($P - S_1$ and $P - S_2$ conversion points). Additionally, it can be used multicomponent seismic records with 3-D sources and 3-D geophones able to generate and record the transversal elastic field (multicomponent seismic). If the whole elastic field is included in the source and it is performed in multicomponent surveys and in addition to petrophysics analysis considering vertical seismic profiles and Crosswell geometries, the quantity of information to be processed increases considerable and any theoretical tool available helps in the task of imaging the subsurface with smaller error percentage.

Corresponding author e-mail: pcontreras@mailfence.com

Historically, most of the seismic signal anisotropic processing analysis done has been based on the Thomsen parametrization (Thomsen, 1986) or the derivations from it that consider azimuthally dependence of the wave field (Tsvankin and Grechka, 2011). Henceforth, the second point to consider is theoretical, and addresses which variables and approximation will be used to solve the Christoffel equation (Grechka, 2017). This depends on the first factor since the acquisition of seismic data depends on what approximation is used to solve the velocity elastic field or the inverse estimation of the elastic stiffnesses.

On the other hand, the solution of the Christoffel equation in oil and gas shale reservoirs, despite the enormous advance during all these years and which started with the use of the Thomsen analytical approximation for VTI systems (Thomsen, 1986) has evolved over time. One can use the classical solution for the Christoffel equation (Musgrave, 1970) and compute phase variables (velocities and angles) and find group variables (group velocities and angles). That can be done for both acquisition geometries, surface-to-surface, and VSP. The slowness solution is also suitable and serves for both types of acquisition geometries including directly nonhyperbolic moveout analysis (Tsvankin and Grechka, 2011; Grechka *et al*., 1999). These are two common approaches used in the exploration of geophysics for oil and gas purposes. A new theoretical tool was proposed recently, the Christoffel equation in the polarization variables (Grechka, 2020) which is important to mention for future practical applications. Therefore, we have introduced Table 1 with a brief classification of the main theoretical methods to resolve the Christoffel equation and some of the first references to appear in the literature.

Summarizing, rocks can be anisotropic for various reasons such as the presence of fractures or strong lithological changes (Thomsen, 1986; Tsvankin and Grechka, 2011; Grechka and Tsvankin, 1997; Grechka *et al*., 1999). Omitting the presence of anisotropy can cause distortions in seismic imaging that turns into economic losses due to well-location errors. On the other hand, anisotropy can be in some cases the answer to the problems of identifying different types of lithology. Therefore, the characterization of anisotropy by estimating elastic constants is essential for the development of velocity estimation techniques, modeling, and 2-D and 3-D seismic processing in order to reduce exploration risk.

In this work, we outline the theoretical computational work performed using the ellipsoidal orthorhombic approximation that was introduced years ago (Contreras *et al*., 1997, 1998). We show how to use their azimuthal dependence and also the way they are visualized in the symmetry vertical planes of orthorhombic media with their main implications as one more approximation to the complex field of elastic wave propagation in low symmetry systems. Finally, we give a theoretical conversion $P - S_i$ point derivation for the ellipsoidal orthorhombic case that can be used in anisotropic signal processing.

Table 1. The different solutions for the eigenvalues of the Christoffel equation using the normal wave front, the slowness, and the polarization vector.

Eigenvalues of the Christoffel equation for phase velocities $\Gamma(\mathbf{n})$ as function of the wave front normal vector **n.** These eigenvalues can be used for both types of acquisition geometries (Grechka, 2017; Musgrave, 1970; Thomsen, 1986).
Eigenvalues of the Christoffel equation $\Gamma(\mathbf{p})$ for phase slowness **p.** These eigenvalues can be used for both kinds of acquisition geometries (Tsvankin and Grechka, 2011; Grechka *et al*., 1999).
Eigenvalues of the Christoffel matrix $\Gamma(\mathbf{U})$ for the polarization vector **U** when they are considered as variables of the phase slowness function $\mathbf{p}(\mathbf{U})$ (Grechka, 2020).

Ellipsoidal seismic velocities in orthorhombic media for vertical seismic profiles

The analysis using the normal moveout velocities was started years ago. It proposed a wave equation based on normal moveout velocities (Stovas, 1998). The use of elliptical seismic velocities was widely used for isotropic and anisotropic media (Levin, 1978; Byun, 1982; Muir, 1990; Dellinger, 1991). Furthermore, in (Contreras *et al*., 1997) it was shown that using a Taylor expansion near the vertical planes of symmetry for an orthorhombic elastic media, one can approximate the whole elastic field obtaining theoretical expressions for the phase and group seismic velocities and angles near the two vertical axes using Silicon graphic stations for their visualization. Sometime later, the work was validated using an inversion procedure (Contreras *et al*., 1998) to obtain the elastic constants for the Cracked Greenhorn Shale (Dellinger, 1991), and was considered of practical interest to test vertical seismic profiles acquisitions in orthorhombic media. That procedure was performed with the help of the eigenvalues of the Christoffel equation $\Gamma(\mathbf{n})$ using the wave front normal vectors **n** with azimuthal dependence following the book by Musgrave (1970) and the idea between the phase and group velocities developed in (Muir, 1990) comparing with the classical approach where the determinant $F = \mathrm{Det}(\Gamma_{ik}(\mathbf{n}) - \rho V^2 \delta_{ik}) = 0$ allows to resolve for the phase velocities (Musgrave, 1970).

Sometime later, Grechka and Tsvankin (1997) pointed out to the author of this work that the same procedure can be obtained using the eigenvalues of the Christoffel equation

using the eigenvalues of the Christoffel equation Γ(**p**) for the phase slowness **p,** with several advantages (Hao and Stovas, 2014). Among them, the eigenvalues of the slowness vector **p** can be used for both kinds of acquisition geometries by means of the Taylor expansion that allows hyperbolic or nonhyperbolic normal moveout analysis using the second or the fourth derivative terms where the azimuthal variables are explicit functions of the vertical slowness q of equation (1). Henceforth, following the general expansion for low symmetry elastic systems with azimuthal dependence in terms of the slowness, the general equation is written as a Taylor expansion (Hao and Stovas, 2014):

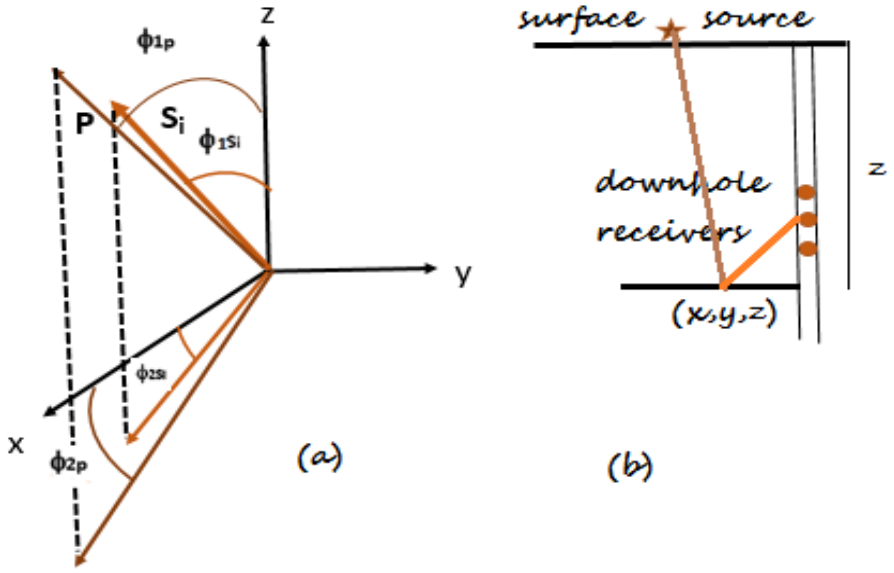

Fig. 1. The elastic response impulses with their respective azimuthal and polar angles in panel (a). Panel (b) corresponds to the vertical seismic profile with incident *P* response impulses and reflected S_i response impulses.

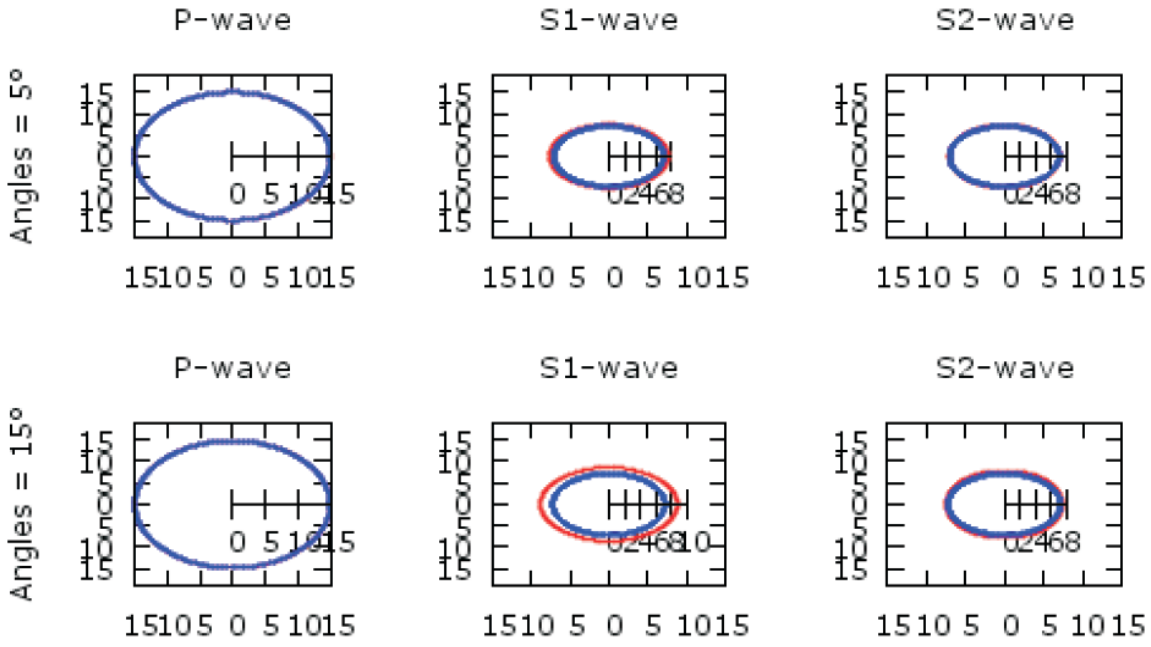

Fig. 2. The azimuthal numerical calculation of the three group velocities (response impulses) in orthorhombic media according to (Contreras *et al*., 2014) for two values of the polar angle in the case of the Cracked Greenhorn Shale using the exact solution (blue color) and the ellipsoidal approximation (red color). The main difference is observed for the transversal elastic mode S_1 when the polar angle is 15°.

$$q(p_x, p_y) \backsimeq q^0 + q_i^0\, p_i + \frac{1}{2}\, q_{ij}^0\, p_i\, p_j + \frac{1}{6}\, q_{ijk}^0\, p_i\, p_j\, p_k + \frac{1}{24}\, q_{ijkl}^0\, p_i\, p_j\, p_k\, p_l \quad (1)$$

where q is the vertical slowness p_z as a function of the horizontal slowness p_x and p_y. In this way, the use of the Christoffel equation $\Gamma(\mathbf{n})$ as function of the wave normal vector **n** (Musgrave, 1970) and the Christoffel equation $\Gamma(\mathbf{p})$ as function of the slowness vector **p** (Hao and Stovas, 2014) resulted equivalent in the direct (Stovas, 1998) and inverse (Levin, 1978) analysis of vertical seismic profiles in orthorhombic elastic media near the vertical axis of symmetry and with azimuthal angular dependence. The expression for the derivatives of second order is given by the following equation (Hao and Stovas, 2014):

$$q_{ij}^0 = \frac{\partial^2 q}{\partial p_i \partial p_j} = -\frac{F_{pi\,,pj} + F_{pi\,,q}\, q_j + F_{pj\,,q}\, q_i + F_{q,q}\, q_i\, q_j}{F_q} \quad (2)$$

where F as function of slowness is given by the following determinant:

$$F = Det\,[C_{ijlk}\, p_j p_l - \delta_{ik}] = 0$$

and the general relation for the slowness vector in term of the phase elastic velocities is:

$$\boldsymbol{p} = (p_1, p_2, q) = V^{-1}(\theta_1, \theta_2)\, \boldsymbol{n}$$

In this case the odd terms, $q^0{}_i = q^0{}_{ijk} = 0$ and nonhyperbolic $q^0{}_{ijkl}$ moveout, have to be neglected in the analysis performed below.

In (Contreras *et al*., 2014), using equations (1) and (2), we were able to visualize the approximate solution for two azimuthal angles in orthorhombic media for the three response impulses using the slowness approach numerically of equation (1) and the general solution of the Christoffel equation in terms of the normal vector for the Cracked Greenhorn Shale (Levin, 1978). Figure 1 schematically shows the elastic response impulses with their respective azimuthal and polar angles. Figure 2 shows the results, where it can be seen that the transversal response impulse S_2 has different solution depending on the parameters in equation (1) (blue ellipse) or the general exact solution (red ellipse) as is explained below. The other elastic modes (namely the P and $S_{2/SH}$ response impulses) are well approximate in this case using the slowness approach (units for the elastic stiffnesses are given in the CGS units [g/(cm × s^2)] and the density ρ = 1 [g/cm^3]):

$$C_{ijlk} = \begin{pmatrix} 336.56 & 117.27 & 103.32 & 0 & 0 & 0 \\ 117.27 & 310.00 & 92.27 & 0 & 0 & 0 \\ 103.32 & 92.27 & 223.95 & 0 & 0 & 0 \\ 0 & 0 & 0 & 49.09 & 0 & 0 \\ 0 & 0 & 0 & 0 & 54.00 & 0 \\ 0 & 0 & 0 & 0 & 0 & 96.36 \end{pmatrix}$$

In particular, we used one general expression that condensed the three elastic fields, namely the longitudinal (P) and the two transversal modes (S_1 and S_2 called sometimes the shear-vertical S_{SV} and shear-horizontal S_{SH}, respectively). Using the Voigt notation that changes the indices of the fourth order elastic tensor "*ijlk"* by the new ones *"ij"*, one has (Contreras *et al*., 1997, 1998):

$$\frac{1}{W_i(\phi_{1,i}, \phi_{2,i})} = \frac{1}{W_{i,z}}\,[\cos\phi_{1,i}]^2 + [\sin\phi_{1,i}]^2 \left\{ \frac{1}{W^i_{NMO,[xz]}}\,[\cos\phi_{2,i}]^2 + \frac{1}{W^i_{NMO,[yz]}}\,[\sin\phi_{2,i}]^2 \right\} \quad (3)$$

where W_i correspond to the square of the group velocities times the density ρ of the medium as function of the group polar (first sub-index 1) azimuthal (second sub-index 2) angles ϕ_I according to Figure 1 panel (a) and $W_i(\phi_{1,i}, \phi_{2,i}) = \rho v_i{}^2(\phi_{1,i}, \phi_{2,i})$ with the symbol i representing the three modes, $i = P$, S_1 or S_2. Figure 1 (general schematic results where P response impulses are shown in brown color and S_i modes in yellow color) shows the group angles and velocities (left *a*-panel) and the use in VSP profiles with "*P*-S_i" conversion points at subsurface interface with coordinates (*x*, *y*, *z*) (right *b*-panel).

The normal moveout coefficients in the form of equation (3) are respectively in the case of orthorhombic symmetry (Contreras *et al*., 1997, 1998):

$$W^P_{NMO,xz} = c_{55} + \frac{(c_{13} + c_{55})^2}{(c_{33} - c_{55})}, \qquad W^P_{NMO,yz} = c_{44} + \frac{(c_{23} + c_{55})^2}{(c_{33} - c_{44})} \quad (4)$$

$$W^{S1}_{NMO,xz} = c_{66}, \qquad W^{S1}_{NMO,yz} = c_{22} + \frac{(c_{23} + c_{44})^2}{(c_{44} - c_{33})} \quad (5)$$

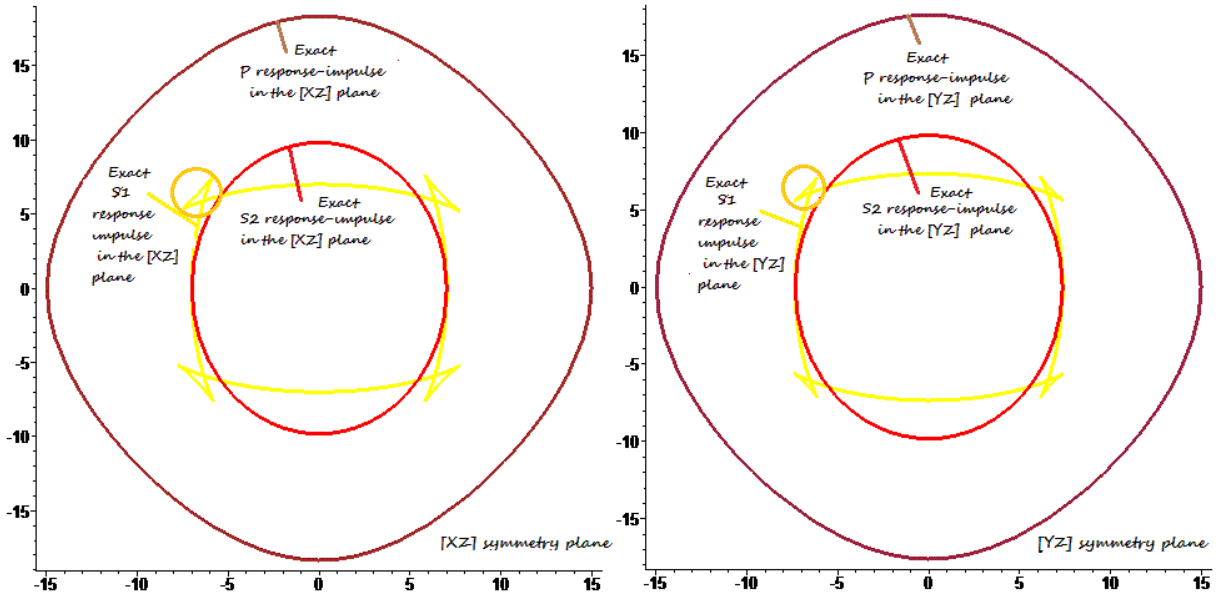

Fig. 3. The exact solution of the Greenhorn shale case in the vertical planes of symmetry for a homogeneous orthorhombic anisotropy.

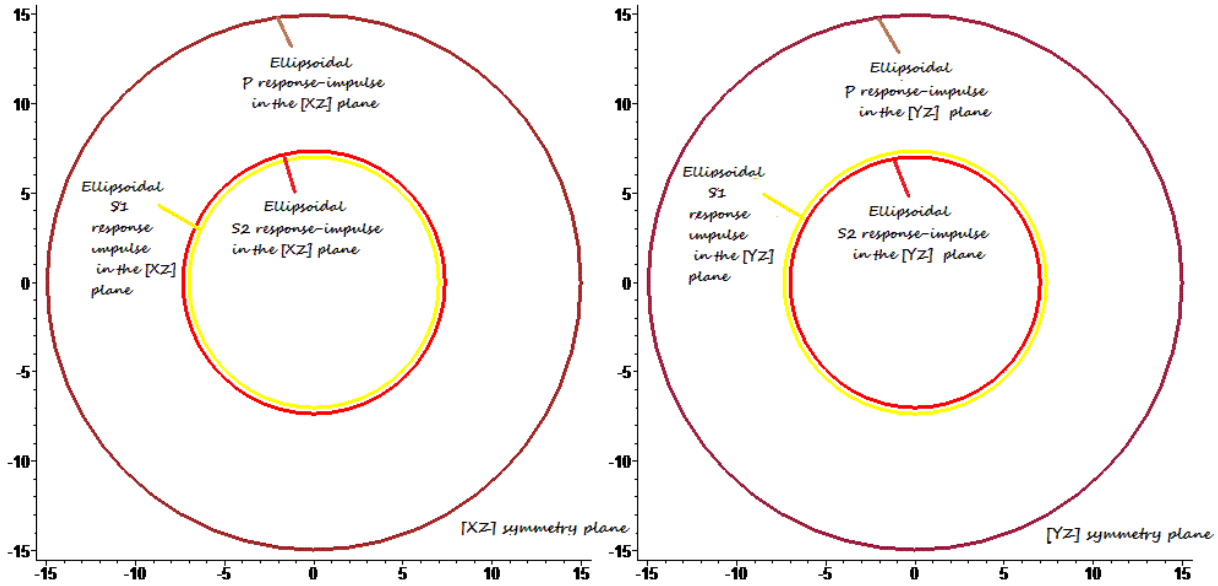

Fig. 4. The ellipsoidal approximation using the same elastic stiffnesses of Figure 3. Notice the difference in the response impulses S_1 and S_2 where the group velocity S_1 is smaller than S_2 if the stiffness C_{13} has a bigger value in the [XZ] plane.

and

$$W_{NMO,xz}^{S2} = c_{11} + \frac{(c_{13} + c_{55})^2}{(c_{55} - c_{33})}$$
$$W_{NMO,yz}^{S2} = c_{66} \qquad (6)$$

The results of azimuthal comparation for the three orthorhombic modes using equations (4)-(6), and the exact solution given in (Musgrave, 1970) by the expression $v_{gi} = c_{ijkl}\alpha_j\alpha_k\beta_l/W_i^{1/2}$, where the W_i are the square phase velocities, the c_{ijkl} are the elastic constants, the α_j and α_k are the eigenvectors, and β_l is the normal direction were shown in Figure 2.

The corresponding VTI elastic media analysis of elliptical dependence on the velocity and the elastic constant inversion was realized in (Michelena, 1994).

In general, one can resolve the Christoffel equation using the eigenvalues of the phase velocities of $\Gamma(\mathbf{n})$ matrix as a function of the wave front normal vector $\mathbf{n}$ for each

vertical plane of symmetry, namely, the [XZ] and the [YZ] planes (the horizontal [XY] plane won't be considered in this case but in (Contreras *et al*., 1998) it is given the procedure on how to solve for the [XY] case. We can do it using the Cracked Greenhorn shale (Levin, 1978) separating the corresponding matrix for each vertical symmetry plane using the exact solution and the correspondent ellipsoidal approximation. The results are given in Figures 3 and 4.

Let us write the elastic matrix elements $C_{\alpha\beta}$ in the Voigt notation. The orthorhombic group has nine independent elastic constants C_{11}, C_{22}, C_{33}, C_{44}, C_{55}, C_{66}, C_{12}, C_{13}, C_{23} plus the three no diagonal depending ones given by the symmetric identity $C_{\alpha\beta} = C_{\beta\alpha}$, i.e. C_{21}, C_{31}, C_{32} making twelve in total (Musgrave, 1970). It makes a complicated numerical solution for response impulses for the whole set that were visualized in (Contreras *et al*., 1997, 1998) since we have to solve for both the polar and azimuthal group angles.

In the case of a hexagonal (VTI medium), one has however five components for the [XZ] vertical plane, i.e. C_{11}, C_{33}, C_{44}, C_{66} and the nondiagonal ones C_{13} and the element $C_{12} = C_{11} - 2C_{66}$. This case can be solving in a rather less complicated eigenvalues form than the orthorhombic one since one has a unique polar angle with respect to the vertical axis of symmetry (Musgrave, 1970). The [YZ] vertical plane is represented by the stiffnesses C_{22}, C_{33}, C_{55}, C_{66} and the nondiagonal ones C_{23} and the element $C_{12} = C_{22} - 2C_{66}$. All values are taken from the Cracked Greenhorn shale (Levin, 1978) orthorhombic set of fractures. We visualize independently for each vertical symmetry plane using an algebraic solver. The [XZ] and [YZ] solutions with the Greenhorn shale partial matrices are represented in Figure 3 for both the symmetry planes.

The main difference for the Greenhorn shale simulation of the three exact elastic response-impulses according to the results shown in Figure 3 are seen mainly in the S_2 component where the triplication defined as three different values of the S_2 group velocities with a fixed polar group angles around 45 degrees are more noticeable in the [XZ] than in the [YZ] symmetry plane, see both orange circles in the right and left planes of Figure 3. This qualitative is explained because in the panel a, the elastic constant that controls the triplication has a value of C_{13} = 103.3 [g/(cm × s^2)] meanwhile the stiffness that control the triple S_2 response impulse value in the [YZ] plane C_{23} = 93.3 [g/(cm × s^2)], i.e. $C_{13} >= C_{23}$.

In the case of the ellipsoidal approximation (Contreras *et al*., 1997, 1998), the same calculations with equations (4)-(6) are shown in Figure 4. It can be seen that for the case of the right panel in Figure 4 representing the ellipsoidal case of the [XZ] symmetry plane and where the elastic constant C_{13} is bigger and gives an augmented exact solution triplication the approximation fails and the S_1 response impulse is calculated with almost not accuracy given values on the whole plane smaller than the S_2 response impulse. This is also seen in Figure 8 of (Contreras *et al*., 1998) when the relative error in the inversion of C_{13} is bigger and constant for the whole range of azimuthal group angles. In the [YZ] plane of symmetry, where the elastic constant C_{23} is smaller and gives a smaller exact solution triplication the approximation works fairly well and the S_1 response impulse is calculated with certain accuracy given values on the whole plane bigger than the S_2 response impulse (right panel in Figure 4). Finally, this is also seen in Figure 9 of (Contreras *et al*., 1998) when the relative error in the inversion of C_{23} is smaller than the case for C_{13}. The relative error increases for the azimuthal group angles variation explaining the conjecture that emerged with the ellipsoidal approximation in the year 1998, when the inversion of the elastic constants was made for the first time using the ellipsoidal approximation (Contreras *et al*., 1998) with respect to the differences in the inversion of C_{13} and C_{23}.

Based on the previous analysis one can see why the ellipsoidal approximation works well in case of the cracked Greenhorn shale with small elastic stiffnesses C_{13} and C_{23} and it can finally define the ellipsoidal orthorhombic approximation as the one that works well in VSP geometries with small elastic stiffnesses C_{13} and C_{23} and where the vertical symmetry planes set close to one another for cracked perpendicular homogeneous media.

Kinematical derivation of the conversion point in orthorhombic media near the vertical axis of symmetry

On the other hand, seismic velocity analysis represents one of the most widely used processing techniques for the treatment of geophysical seismic data in the oil and gas industry. A method of acquisition commonly used is the Common-Mid-Point (CMP) method. The general idea of this method is to acquire a series of traces (gather) which reflect from the same common subsurface mid-point. Similarly, to group seismic traces of multicomponent signals under the CMP criterion, an expression for the conversion point of each of the traces can be used to group those that have the same CMP. General expressions were developed previously for the calculation of the conversion of *"P-S$_i$"* points in isotropic (Fromm *et al*., 1985), vertical transverse isotropy VTI (Sena and Toksöz, 1993), horizontal transversal isotropy HTI (Hao *et al*., 2013) and orthorhombic media (Xu and Stovas, 2019) with the goal of seismic exploration analysis.

However, these expressions can be simplified when it comes to performing analysis in a medium with azimuthal anisotropy such as fractured orthorhombic media with dependency of several elastic stiffness. In general, azimuthally elastic depend media such as the HTI, the orthorhombic and the monoclinic ones, are those with combinations of multiple vertical fracture sets and possible horizontally fine layering, they are of great importance for fracture characterization (Tsvankin and Grechka, 2011).

Therefore, it is convenient to obtain expressions for the coordinates of the conversion "*P*-S_i" point considering azimuthal variations of the velocity for any mode of propagation for specific acquisition geometries such as VSP. It will be shown how to apply a particular methodology developed for VTI media (Sena and Toksöz, 1993) to derive asymptotic 3-D analytic expressions for the conversion point in orthorhombic media within the ellipsoidal approximation (Contreras *et al.*, 1997, 1998) for the *P*-S_1 and *P*-S_2 modes. We should note that such expressions will be valid near a single axis of symmetry, such that, those with large "depths" and small "offsets", which represents practical cases encountered in seismic velocity analysis for vertical seismic profiles and where the *Z* location of the surface source and the downhole receiver is known.

Let us consider the case of a general homogeneous elastic medium with orthorhombic symmetry and a particular density that for simplicity we fixed equal to 1 [g/cm^3], as shown in Figure 5 where the two vertical planes [XZ] and [YZ] and the ellipsoidal group velocities will be combined with the help of a trigonometric analysis, the used of the Fermat theorem and the derivation of travel times following Sena and Toksöz (1993), arriving to analytical expressions of the conversion point in the ellipsoidal anisotropic case.

In Figure 5, it can be seen that for the incident *P* response-impulse, the following equations are true as function of the response-impulse polar (denoted by index 1) and response-impulse azimuthal angles (denoted by index 2):

$$\cos^2\phi_{1P} = \frac{Z^2}{Z^2 + {X_j}^2 + {Y_j}^2}, \sin^2\phi_{1P} = \frac{{X_j}^2 + Y_j^2}{Z^2 + {X_j}^2 + {Y_j}^2}, \quad \cos^2\phi_{2P} = \frac{X_j^2}{{X_j}^2 + {Y_j}^2}, \quad \sin^2\phi_{2P} = \frac{Y_j^2}{{X_j}^2 + {Y_j}^2} \tag{7}$$

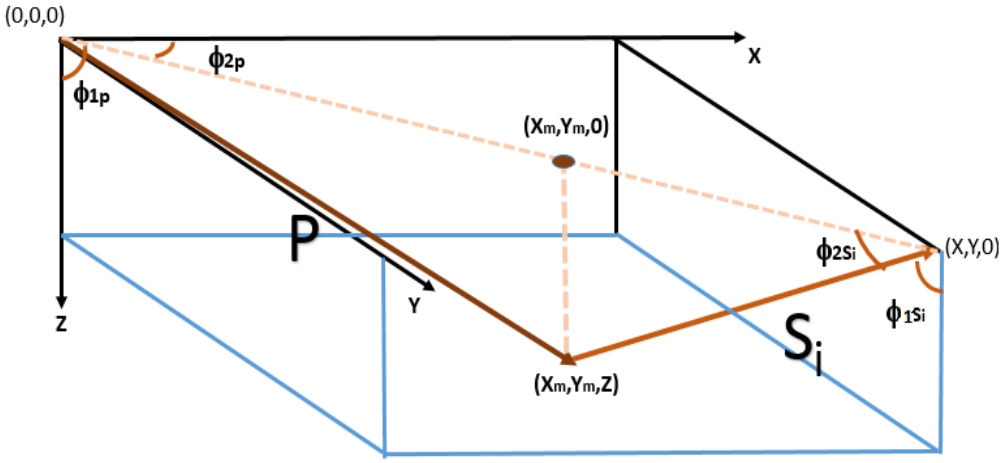

Fig. 5. The general scheme of the *P*-S_i conversion point on a 3-D line in a homogeneous anisotropic medium with orthorhombic symmetry.

It can be also written down for the reflected shear response-impulses (S_i with the index i = 1 or SV, and or 2 or SH). It follows that as a function of the corresponding shear azimuthal angles that control the response impulse in the horizontal plane [XY] one has

$$\cos^2\phi_{1Sj} = \frac{Z^2}{Z^2 + (X - X_j)^2 + (Y - Y_j)^2}, \quad \sin^2\phi_{1Sj} = \frac{(X - X_j)^2 + (Y - Y_j)^2}{Z^2 + (X - X_j)^2 + (Y - Y_j)^2} \tag{8}$$

By the geometrical congruence of similar triangles, it follows that $\phi_{2P} = \phi_{2Sj}$ and therefore, the following relationship takes place:

$$\cos^2\phi_{2Sj} = \cos^2\phi_{2P} = \frac{X_j^2}{{X_j}^2 + {Y_j}^2}, \quad \sin^2\phi_{2Sj} = \sin^2\phi_{2P} = \frac{Y_j^2}{{X_j}^2 + {Y_j}^2} \tag{9}$$

For equations (8) and (9), j = 1, 2 are the two propagation modes S_1 and S_2, respectively; ϕ_{1Sj} and ϕ_{2Sj} and are the

polar and azimuthal group angles for the propagation modes S_j.

The kinematic travel time analysis procedure is used a continuation with the aim of the Fermat theorem (Sena and Toksöz, 1993). The expression that determines the travel time of the incident wave P and reflected wave S_j is the sum of the two travel times $T = T_{Pi} + T_{Sj}$, where each travel time corresponds to the expressions to be derived using the notation from the previous section and Figure 5, where T_{Pi} is the travel time from the incident P_i wave and T_{Sj} is the travel time for the reflected S_j wave. Considering elementary trigonometry and looking at the general scheme shown in Figure 5, an expression for both travel times, i.e. T_{Pi} and T_{Sj} as function of the group angles and the elastic constants can be conveniently written as

$$T_{Pi} = \frac{Z}{V_{P(\emptyset_{1P},\emptyset_{2P})}\cos\emptyset_{1P}}, T_{Sj} = \frac{Z}{V_{Sj\,(\emptyset_{1Sj},\emptyset_{2Sj})}\cos\emptyset_{1sj}}$$

where V_P and V_{Sj} are the response impulses (group velocities) for the propagation longitudinal and transversal elastic modes, respectively, where by means of some straightforward but lengthy algebra a more suitable for the analysis in orthorhombic fracture media near the vertical axis expression for the converted P-S_i modes are derived.

The square of the response-impulses as function of the azimuthal angles can be given by the mathematical expression:

$$W_{gi}^{-1}(\emptyset_{1,i},\emptyset_{2,i}) = C_0^i + C_1^{''i}(\emptyset_{2,i})\sin^2\emptyset_{1,i}$$

where $C_0{}^i$ is related to the velocity of propagation in the vertical axis, and $C_1{}^{''i}$ has the following anisotropic dependence form in the ellipsoidal case:

$$C_1^{''i}(\emptyset_{2,i}) = W_{NMO[x,z]}^{-1,i} - W_z^{-1,i} + (W_{i,NMO[y,z]}^{-1} - W_{i,NMO[x,z]}^{-1})\sin^2\emptyset_{2,i}$$

Taking into account the mathematical expression for the different propagation modes developed in the previous paragraphs and considering that the group polar angles are small but the azimuthal angles can have any allowed value in the horizontal plane, the travel times expressions for longitudinal and transversal response-impulses in ellipsoidal orthorhombic elastic media can be written using the geometry considerations sketched in Figure 5.

Henceforth, for the P wave response impulse the incident 3-D azimuthal travel time takes the following form:

$$T_{Pi} = \frac{1}{4\sqrt{C_0^P}Z}(2Z^2 + X_1^2 + Y_1^2)\left(2C_0^P + C_1^{''P}\sin^2(\emptyset_{1,p})\right) \quad (10)$$

and also, for the S_1 and S_2 transversal response impulses, the reflected travel times are given according to

$$T_{Sj} = \frac{1}{4\sqrt{C_0^s}Z}(2Z^2 + (X - X_1)^2 + (Y - Y_1)^2)\left(2C_0^s + C_1^{''s}\sin^2(\emptyset_{1,s})\right. \quad (11)$$

Once an approximate expression of the ray paths travel times of the different response impulses have been obtained, the conversion point can be found, using Fermat's theorem of the minimum time considering that in general one has $(X_j, Y_j) < (X, Y)$.

In the ellipsoidal orthorhombic elastic case, we start from the Fermat theorem for each horizontal azimuthal component $\partial T/\partial X_j = \partial T/\partial Y_j = 0$. On the other hand, for the Z direction, the velocity is constant, we suppose that the depth Z is known (particularly this is the fact in the case of vertical seismic profiles), and therefore, asymptotic analysis is performed only for the X_j and Y_j components. Taking into account the total horizontal travel time for the three responses impulses and their respectively derivatives using the partial derivatives expression $\partial T/\partial X_j = (\partial T_{Pi}/\partial X_j) + (\partial T_{Sj}/\partial X_j)$, and considering equation (10), the following general expression near the vertical axis is derived after some algebraic manipulations:

$$\frac{\partial T}{\partial X_j} = \frac{1}{Z}\left\{\frac{X_j}{\sqrt{C_0^P}}W_{NMO[x,z]}^{-1,P} + \frac{X_j - X}{\sqrt{C_0^{Sj}}}W_{NMO[x,z]}^{-1,Sj}\right\} = 0,$$

which means that

$$\left\{\frac{X_j}{\sqrt{C_0^P}}W_{NMO[x,z]}^{-1,P} + \frac{X_j - X}{\sqrt{C_0^{Sj}}}W_{NMO[x,z]}^{-1,Sj}\right\} = 0.$$

Solving for X_j, one arrives at the first general expression of one of the conversion point components for orthorhombic ellipsoidal media near the vertical axis of symmetry as function of normal moveout square velocities:

$$X_j = X\frac{\sqrt{C_0^P}W_{NMO[x,z]}^{-1,Sj}}{\sqrt{C_0^P}W_{NMO[x,z]}^{-1,Sj} + \sqrt{C_0^{Sj}}W_{P,NMO[x,z]}^{-1}} \quad (12)$$

Similarly, using $\partial T/\partial Y_j = (\partial T_{Pi}/\partial Y_j) + (\partial T_{Sj}/\partial Y_j)$, multiplying the traveltime derivative by $Z(C_0{}^P C_0{}^{Sj})^{1/2}$, and making the respective factorization, a general expression can be found for the second horizontal component Y_j considering equation (11) to get

$$Y_j = Y\frac{\sqrt{C_0^P}W_{NMO[y,z]}^{-1,Sj}}{\sqrt{C_0^P}W_{NMO[y,z]}^{-1,Sj}+\sqrt{C_0^{Sj}}W_{NMO[y,z]}^{-1,P}} \quad (13)$$

In this way, it has been possible to obtain asymptotic expressions for the coordinates of the conversion point for a medium with orthorhombic elliptical anisotropy considering azimuthal group angle variations that represents a perpendicular set of fractures.

The specific form of the horizontal coordinates in the [XY] plane for the conversion point in an orthorhombic medium for the conversion form is the following (X_1, Y_1) pair for the P-S_1 conversion point:

$$X_1 = X\frac{\sqrt{C_0^P}W_{NMO[x,z]}^{-1,S1}}{\sqrt{C_0^P}W_{NMO[x,z]}^{-1,S1}+\sqrt{C_0^{S_1}}W_{NMO[x,z]}^{-1,P}}$$
$$Y_1 = Y\frac{\sqrt{C_0^P}W_{NMO[y,z]}^{-1,S1}}{\sqrt{C_0^P}W_{,NMO[y,z]}^{-1,S1}+\sqrt{C_0^{S_1}}W_{NMO[y,z]}^{-1,P}} \quad (14)$$

For the P-S_2 conversion point analogously we find the following (X_2, Y_2) pair:

$$X_2 = X\frac{\sqrt{C_0^P}W_{NMO[x,z]}^{-1,S2}}{\sqrt{C_0^P}W_{NMO[x,z]}^{-1,S2}+\sqrt{C_0^{S_2}}W_{NMO[x,z]}^{-1,P}}$$
$$Y_2 = Y\frac{\sqrt{C_0^P}W_{NMO[y,z]}^{-1,S2}}{\sqrt{C_0^P}W_{NMO[y,z]}^{-1,S2}+\sqrt{C_0^{S_2}}W_{NMO[y,z]}^{-1,P}} \quad (15)$$

This is important for different reasons such as the analysis of seismic data acquired in multicomponent VSP surveys that is crucial for the correct interpretation of the data (positioning of events and imaging). Physically in the interface where the conversion occurs, the energy carried by the longitudinal response-impulse is converted into energy carried now by the transversal modes.

One way to corroborate the general validity of these results is the reduction from equations (14) and (15) to the isotropic limit (Fromm *et al*., 1985). For the isotropic case, we have that for the longitudinal response impulses it follows that the new normal moveout square velocities are

$$W_{P,NMO[x,z]}^{-1} = W_{P,NMO[y,z]}^{-1} = C_0^P = \frac{1}{V_P^2}$$

For the transversal elastic modes, one has that the square of the normal moveout velocities is reduced to

$$W_{Sj,NMO[x,z]}^{-1} = W_{Sj,NMO[y,z]}^{-1} = C_0^{Sj} = \frac{1}{V_S^2}$$

Replacing those expressions back in equations (14) and (15), one finally obtains

$$(X_j, Y_j) = \left(X\frac{1}{1+\frac{V_S}{V_P}}, Y\frac{1}{1+\frac{V_S}{V_P}}\right)$$

which are the well-known expressions for an isotropic elastic medium (Fromm *et al*., 1985).

CONCLUSION

First, we conclude that simple analytical expressions using the Fermat theorem and for practical multi-walkaway velocity analysis such as in vertical seismic profiles of the conversion "P - S_i" points that belong to a single interface in orthorhombic ellipsoidal elastic media with general azimuthal dependence (including near offsets and small polar angles) were derived and compared with the isotropic case.

Second, we explain the difference in the inversion of the elastic constants C_{13} and C_{23} within the ellipsoidal approximation (Contreras *et al*., 1998) with respect to the differences in the growth of the azimuthal angle. The relative error in the inversion of C_{13} remained constant for azimuthal angle values between 0° and 90°. Meanwhile, the relative errors in the inversion of the stiffness C_{23} increased with the growth of the azimuthal angle (see in Figures 7 and 8 in (Contreras *et al*., 1998) respectively). We find that is due to the size of the triplication in each vertical symmetry plane and as it can be seen in Figure 3, higher stiffness input values for C_{13} set constant inverted values for arbitrary azimuthal angles and constant higher relative errors.

As additional points, a very brief analysis of the use of the Christoffel equation in different representations with the respective references is mentioned for future works. Finally, we recommend the study of orthorhombic systems using the same methodology as the one represented in (Contreras *et al*., 2019), in particular, to observe the P response impulse with imaging purposes implementing perfect matched layer boundary conditions, staggered finite-difference grid 3-D schemes, and Valgrind's memcheck, to simulate a 3D elastic wave generating synthetic seismograms and screenshots. We also point out the inclusion of pressure for studies and visualization in anisotropic media using VSP profiles with downhole receivers as the one represented in (Guerrero, 2022). My notes on the prediction of pressure induce phonon instabilities via computational modelling of

Acoustic wave propagation in isotropic and anisotropic crystals. DOI: https://doi.org/10.13140/RG.2.2.34112.81925).

ACKNOWLEDGEMENT

The author the support and research discussions in Intevep SA, the Research branch of Petroleos de Venezuela from the years 1995 to 1998.

REFERENCES

Byun, BS. 1982. Seismic parameters for media with elliptical velocities dependencies. Geophysics. 47(12):1621-1626. DOI: https://doi.org/10.1190/1.1441312

Contreras, P., Klíe, H., Mora, C. and Michelena, R. 1997. Ellipsoidal Approximation of Velocities in Orthorhombic Media. European Association of Geoscientists and Engineers. Conference Proceedings, 5th International Congress of the Brazilian Geophysical Society. November 1997, cp-299-00087. DOI: https://doi.org/10.3997/2214-4609-pdb.299.87

Contreras, P., Klíe, H. and Michelena, RJ. 1998. Estimation of elastic constants from ellipsoidal velocities in orthorhombic media. SEG Technical Program Expanded Abstracts 1998. pp.1491-1494. DOI: https://doi.org/10.1190/1.1820194.

Contreras, P., Grechka, V. and Tsvankin, I. 1999. Moveout inversion of *P*-wave data for horizontal transverse isotropy. Geophysics. 64(4):1219-1229. DOI: https://doi.org/10.1190/1.1444628.

Contreras, P., Rincon, L. and Burgos, J. 2014. Ellipsoidal response-impulses in fracture media. The 12th International Congress on Numerical Methods in Engineering and Applied Sciences (CIMENICS 2014). I:25-30. DOI: https://doi.org/10.48550/arXiv.1812.09125.

Contreras, P., Larrazábal, G. and Florio, C. 2019. Perfectly matched layers' simulation in two-dimensional media. Canadian Journal of Pure and Applied Sciences. 13(3):4861-4867.

Dellinger, JA. 1991. Anisotropic seismic-wave propagation. Ph.D. Thesis, Stanford University, Stanford, California, USA.

Fromm, G., Krey, T. and Wiest, B. 1985. Static and dynamic correction. In: Seismic Shear Waves. Handbook of Geophysical Exploration. Ed. Dohr, G. Geophysical Press. 15b:191-225.

Grechka, V. 2017. Algebraic degree of a general group-velocity surface. Geophysics. 82(4):WA45-WA53. DOI: https://doi.org/10.1190/geo2016-0523.1

Grechka, V. 2020. Christoffel equation in polarization variables. Geophysics. 85(3):C91. DOI: https://doi.org/10.1190/geo2019-0514.1.

Grechka, V. and Tsvankin, I. 1997. Moveout velocity analysis and parameter estimation for orthorhombic media. SEG Technical Program Expanded Abstracts. 1226-1229. DOI: https://doi.org/10.1190/1.1885619.

Grechka, V., Contreras, P. and Tsvankin, I. 1999. Inversion of normal moveout for monoclinic media. SEG Technical Program Expanded Abstracts. 1883-1886. DOI: https://doi.org/10.1190/1.1820913

Hao, Q. and Stovas, A. 2014. Anelliptic approximation for *P*-wave phase-velocity in orthorhombic media. 16th International Workshop on Seismic Anisotropy (16IWSA), Natal, Brazil. DOI: https://doi.org/10.13140/2.1.3970.8488.

Hao, Q., Stovas, A. and Alkhalifah, T. 2013. The azimuth-dependent offset-midpoint travel time pyramid in 3D HTI media. SEG Technical Program Expanded Abstracts. 3335-3339. DOI: https://doi.org/10.1190/segam2013-0058.1.

Levin, FK. 1978. The reflection, refraction and diffraction of waves in media with elliptical velocity dependence. Geophysics. 43(3):528-537. DOI: https://doi.org/10.1190/1.1440833.

Michelena, RJ. 1994. Elastic constants of transversely isotropic media from constrained aperture travel times. Geophysics. 59(4):658-667 DOI: https://doi.org/10.1190/1.1443625.

Muir, F. 1990. Various equations for TI media. SEP Stanford. 70:367-372.

Musgrave, MJP. 1970. Crystal Acoustics. Holden Day, San Francisco, USA. pp vii+288.

Sena, A. and Toksöz, N. 1993. Kirchhoff migration and velocity analysis for converted and no converted waves in anisotropic media. Geophysics. 58(2):265-275. DOI: https://doi.org/10.1190/1.1443411.

Stovas, A. 1998. Wave-equation-based normal moveout. Journal of Seismic Exploration. 7(1):1-8.

Thomsen, L. 1986. Weak elastic anisotropy. Geophysics. 51(10):1954-1966. DOI: https://doi.org/10.1190/1.1442051.

Tsvankin, ID. and Grechka, V. 2011. Seismology of azimuthally anisotropic media and seismic fracture characterization. Society of Exploration Geophysicists. pp 510. DOI: https://doi.org/10.1190/1.9781560802839.

Xu, S. and Stovas, A. 2019. Estimation of the conversion point position in elastic orthorhombic media. Geophysics. 84(1):C15-C25. DOI: https://doi.org/10.1190/geo2018-0375.1.

Received: July 25, 2022; Revised: Sept 11, 2022;
Accepted: Sept 17, 2022